Intermetallics 96 (2018) 79–83

Contents lists available at ScienceDirect

Intermetallics

journal homepage: www.elsevier.com/locate/intermet

Amorphous microwires of high entropy alloys with large magnetocaloric effect

Wei Sheng[a,b], Jun-Qiang Wang[b], Gang Wang[a], Juntao Huo[b,*], Xinmin Wang[b], Run-Wei Li[b]

[a] School of Materials Science and Engineering, Shanghai University, Shanghai, 200444, China
[b] Key Laboratory of Magnetic Materials and Devices, Zhejiang Province Key Laboratory of Magnetic Materials and Application Technology, Ningbo Institute of Materials Technology & Engineering, Chinese Academy of Sciences, Ningbo, Zhejiang, 315201, China

ARTICLE INFO

Keywords:
High-entropy alloy
Magnetocaloric effect
Metallic glasses
Microwire

ABSTRACT

Microwires of $Gd_{20}Ho_{20}Er_{20}Al_{20}TM_{20}$ (TM = Fe, Co and Ni) high-entropy metallic glasses (HE-MGs) are successfully fabricated by a melt-extraction method, which exhibit good magnetocaloric properties. The maximum magnetic entropy change and refrigerant capacity under 5 T of the $Gd_{20}Ho_{20}Er_{20}Al_{20}Co_{20}$ HE-MG microwire can reach 10.2 J kg^{-1}K^{-1} and 625 J kg^{-1}, respectively. In addition, the magnetocaloric properties of the HE-MG microwires can be widely tuned by doping different transition metals. The HE-MG microwires combining high heat-exchange efficiency and excellent mechanical properties are attractive candidates for applications in magnetic refrigeration.

Compared with conventional gas refrigerants, magnetic refrigerants based on a magnetocaloric effect (MCE) exhibit better properties, such as higher efficiency and better environmental friendliness [1–5]. In the past decades, many crystalline materials, such as Gd, $Gd_5Si_2Ge_2$ (at. %) and $LaFe_{11.4}Si_{1.6}$, were developed, and demonstrated their potentials for an application as magnetic refrigerants [1–16]. Metallic glasses (MGs), as a kind of second-order magnetic phase transition materials, manifest a large MCE in a wide temperature range owing to their amorphous nature. Furthermore, MGs also exhibit a high electrical resistivity (meaning a small eddy current heating), a high corrosion resistance, outstanding mechanical properties, and a high thermal stability, which are suitable for the application in the magnetic refrigeration. Recently, high-entropy MGs (HE-MGs) are successfully synthesized [6–9]. Different from the conventional MGs that are usually composed of one or two major elements, the HE-MGs are composed of several elements with equimolar concentrations [6–9]. Due to a strong topological and chemical disorder structure, HE-MGs usually exhibit a large magnetic entropy change (ΔS_M), and refrigerant capacity (*RC*), and thus are promising candidates for the magnetic refrigeration [10–12].

Usually, good magnetic refrigerants, working as both cooling agent, and regenerator medium, are expected to possess a large ΔS_M value and a good capability of heat exchange [13]. To obtain an efficient heat transfer, the magnetic refrigerants must have a high surface area. In this case, decreasing the geometric size of the regenerative substance to be micrometer scale, such as micro-sized spherical particles, thin plates or wires, is favourable for the refrigerate properties. Recently, the MCE of MGs in the forms of bulk [14,15], ribbon [16,17], powder [18,19] and wire [20–23] were extensively studied. Significantly, the MG microwires exhibit better MCE [20–23] compared with their bulk and ribbon counterparts, which are mainly attributed to their better adaptability and higher heat-exchange efficiency. Magnetocaloric materials with a diameter of 50–200 μm (the corresponding surface area is about 10,000–40,000 m^2/m^3) exhibit a good heat-transfer capability under an operating frequency of 1 Hz [24,25]. Furthermore, compared with the spherical and plate shapes, the long wires have a negligible demagnetization factor when the magnetic field is applied along the wire direction [26]. Thus, micro-sized wires with the good MCE are desired to improve the efficiency of magnetic refrigeration system.

In this work, $Gd_{20}Ho_{20}Er_{20}Al_{20}TM_{20}$ (TM = Fe, Co and Ni) HE-MG microwires are fabricated successfully by a melt-extraction method, as schematically shown in Fig. 1a. The effect of component, temperature and magnetic field on the magnetic-transition temperature, the magnetic-entropy change, and the refrigerant capacity are investigated. The results show the HE-MG microwires are suitable candidates for the magnetic refrigerants.

The optical image (Fig. 1b), and SEM images (Fig. 1c, d, e) of the $Gd_{20}Ho_{20}Er_{20}Al_{20}TM_{20}$ microwires show that the HE-MG microwires have a diameter of about 60 μm, and a length of several centimetres. Their amorphous structures are confirmed by XRD patterns and DSC traces, as shown in Fig. 2. From the DSC traces, it can be seen that an endothermic glass transition occurs followed by several exothermic crystallization peaks for each alloy, indicating the formation of glassy

* Corresponding author.
E-mail address: huojuntao@nimte.ac.cn (J. Huo).

https://doi.org/10.1016/j.intermet.2018.02.015
Received 27 November 2017; Received in revised form 22 February 2018; Accepted 26 February 2018
0966-9795/

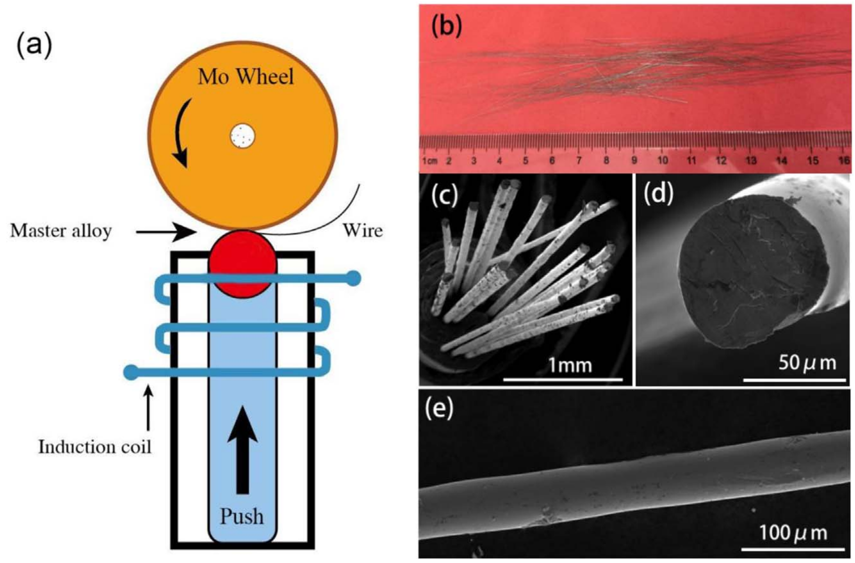

Fig. 1. Experimental setup. (a) The schematic illustration of melt extraction technique, (b) the optical image, and (c), (d), (e) the SEM images of HE-MG microwires.

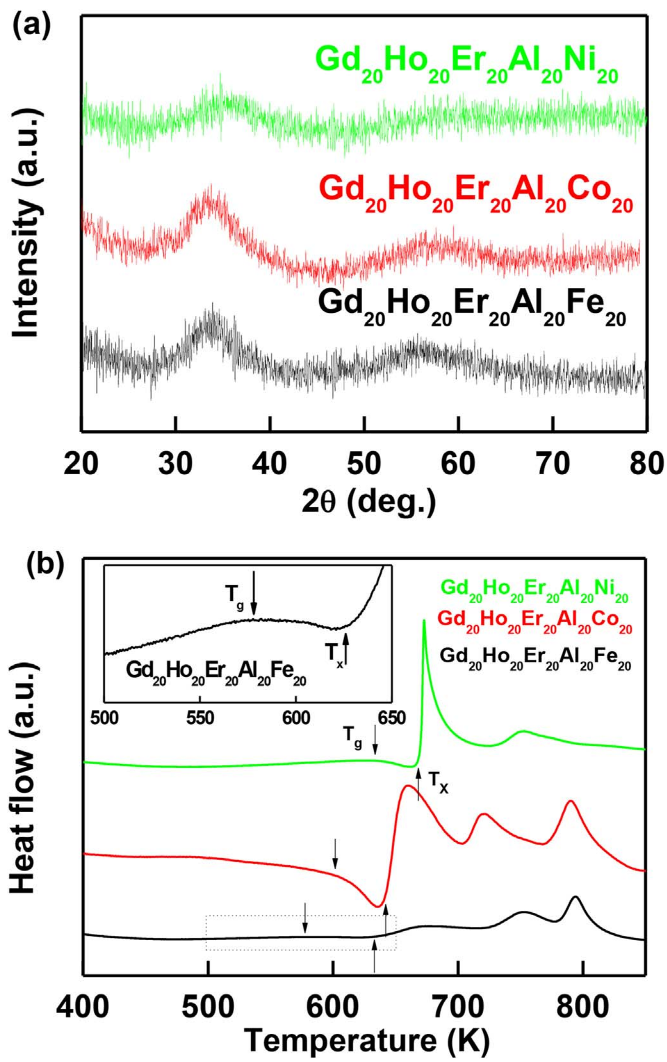

Fig. 2. Structure and thermal properties of $Gd_{20}Ho_{20}Er_{20}Al_{20}TM_{20}$ (TM = Fe, Co and Ni) HE-MG microwires. (a) XRD patterns and (b) DSC traces of HE-MG microwires. The inset shows the magnified DSC trace of $Gd_{20}Ho_{20}Er_{20}Al_{20}Fe_{20}$.

phase. The XRD patterns show a broad diffraction maximum and no sharp Bragg peaks from crystalline phases, which further confirm the amorphous structure. The glass-transition temperature (T_g), first crystallization temperature (T_x) and supercooled-liquid region ($\Delta T_x = T_x - T_g$) are listed in Table 1. A large ΔT_x value suggests a good glass-forming ability (GFA) [27]. The ΔT_x values of these alloys are smaller than those of other rare-earth based MGs, as shown in Table 1, indicating their poor GFA. This may be attributed to the compositions of these HE-MG microwires are deviated from the eutectic points despite their high mixing entropy [10].

The temperature dependence of the magnetization for the HE-MG microwires is measured upon heating under a field of 200 Oe, as shown in Fig. 3a. A spin-freezing transition can be observed in the field cooling (FC) curve. A cusp exists in the zero field cooling (ZFC) curve at the same temperature. The divergence between the FC and ZFC curves is a typical spin-glass-like behavior [28]. The sample of TM = Fe has the widest magnetic-transition temperature (T_C) range among all samples. The T_C values calculated from the differentiation of the FC curves are 55, 39 and 25 K, for the samples of TM = Fe, Co and Ni, respectively, as marked by arrows in the insert of Fig. 3a. Evidently, the T_C value decreases rapidly when TM changes from Fe to Ni. The increase of 3d electrons from Fe ($3d^6$) to Ni ($3d^8$) weakens the magnetic interactions that are dominated by the 3d-electron exchange, and then reduces the exchange energy and the T_C value of the alloys. It is evident that the T_C value can be tuned easily in a large temperature range by alloying different elements in the HE-MG microwire.

To characterize the magnetocaloric effect of these microwires, the ΔS_M values are calculated based on the isothermal-magnetization (*M-H*) curves in a wide temperature range under different external magnetic fields ranged from 0 to 5 T, as shown in Fig. 3b. In an isothermal process of magnetization, the total ΔS_M value of the system caused by a magnetic field (H) can be calculated based on the isothermal *M-H* curves at various temperatures (T_i) using the equation [10],

$$\Delta S_M(T_i, H) = \frac{\int_0^H M(T_i, H)dH - \int_0^H M(T_{i+1}, H)dH}{T_i - T_{i+1}}. \tag{1}$$

Fig. 4a displays the ΔS_M value as a function of the temperature under the magnetic fields of 1, 2, 3, 4 and 5 T for the

Table 1
Properties of the HE-MG microwires developed in this work, and from the reported MGs: the glass transition temperature (T_g), first crystallization temperature (T_x), supercooled liquid region (ΔT_x), magnetic transition temperature (T_C), peak value of the magnetic entropy change ($|\Delta S_M^{pk}|$), full width at half-maximum of the ΔS_M peak (δT_{FWHM}), and refrigerant capacity (RC) under a field of 5 T.

Composition	Form	Tg (K)	Tx (K)	ΔTx (K)	TC (K)	$|\Delta S_M^{pk}|$ ($J\ kg^{-1}\ K^{-1}$)	δT_{FWHM} (K)	RC ($J\ kg^{-1}$)	Ref.
$Gd_{20}Ho_{20}Er_{20}Al_{20}Fe_{20}$	wire	577	631	54	55	5.1	88	446	This work
$Gd_{20}Ho_{20}Er_{20}Al_{20}Co_{20}$	wire	610	647	37	39	10.2	61	625	This work
$Gd_{20}Ho_{20}Er_{20}Al_{20}Ni_{20}$	wire	636	669	33	25	9.5	54	511	This work
$Ho_{20}Er_{20}Co_{20}Al_{20}Gd_{20}$	bulk	612	652	40	37	11.2	56	627	[10]
$Ho_{20}Er_{20}Co_{20}Al_{20}Dy_{20}$	bulk	632	668	36	18	12.6	37	468	[10]
$Ho_{20}Er_{20}Co_{20}Al_{20}Tm_{20}$	bulk	648	680	32	9	15.0	25	375	[10]
$(Ho_{0.3}Er_{0.7})_{55}Al_{27.5}Co_{17.5}$	bulk	658	721	63	10	8.55	19	162.4	[14]
$Gd_{53}Al_{24}Co_{20}Zr_3$	bulk	599	653	54	93	9.4	63	590	[15]
$Gd_{60}Al_{20}Co_{20}$	wire	574	600	26	109	10.1	91	681	[20]
$Gd_{55}Al_{20}Co_{25}$	wire	585	637	52	110	9.7	83	580	[25]

$Gd_{20}Ho_{20}Er_{20}Al_{20}Co_{20}$ HE-MG microwire. Fig. 4b shows the ΔS_M value as a function of the temperature for the $Gd_{20}Ho_{20}Er_{20}Al_{20}TM_{20}$ microwires. The ΔS_M value reaches the peak value near T_C. The peak values of the magnetic-entropy change ($|\Delta S_M^{pk}|$) for the samples at the external field of 5 T reach 5.1 $J\ kg^{-1}K^{-1}$ (TM = Fe), 10.2 $J\ kg^{-1}K^{-1}$ (TM = Co) and 9.5 $J\ kg^{-1}K^{-1}$ (TM = Ni), respectively. These values are already comparable to those of the good magnetocaloric crystalline materials, and apparently larger than those of the rare-earth based MGs, as listed in Table 1. It can be seen that the temperature, and the ΔS_M peak value can be tuned by changing the rare-earth elements. The peak of the ΔS_M value as the function of the temperature shows a severely asymmetrical distribution. With increasing temperature, below T_C, the ΔS_M value rapidly increases to the peak value, and then gradually decreases. This is because the hysteresis is larger below T_C than that above T_C which derives from the strong random-magnetic anisotropy [29]. Another reason is the exchange-interaction frustration associated with the spin-glass frozen behavior due to the disorder structure below T_C. Because of spin rotating with the applied external field, the ΔS_M value becomes very small.

Regarding that the Arrott plot can be used to identify the order of the magnetic-phase transition [2], the slope of M^2 vs. H/M curves can reflect the state of magnetic-phase transition, i.e., the negative slop corresponding to the first-order transition, and the positive slope corresponding to the second-order transition. In Fig. 3c, the positive slopes of the Arrott plots for the HE-MG microwires denote a second-order magnetic transition (SOMT) [30,31]. Furthermore, Franco method ($\Delta S_M \propto H^n$) is also introduced to demonstrate SOMT of these alloys [32–34]. The n values are 0.92, 0.85 and 1.46 at temperatures of below, near, and above T_C, respectively, which can be comparable to the suggested values from the Franco method, and thus confirms their SOMT. The SOMT with gradual and continuous magnetization variation near T_C, exhibiting broad ΔS_M value peaks without the thermal and magnetic hysteresis, is currently considered to be the optimal property for the magnetic refrigerants.

The RC is another important parameter to characterize the efficiency of magnetic refrigerants. The RC value in this work is estimated based on the $|\Delta S_M^{pk}|$, and the full width at half-maximum of the peak, δT_{FWHM} [5]

$$RC_{FWHM} = |\Delta S_M^{pk}| \times \delta T_{FWHM}, \tag{2}$$

The RC_{FWHM} for the samples of TM = Fe, Co and Ni are determined to be 426, 625 and 511 $J\ kg^{-1}$, respectively. Interestingly, the RC_{FWHM} value of the $Gd_{20}Ho_{20}Er_{20}Al_{20}Co_{20}$ HE-MG microwire is equal to the value of the bulk counterpart (627 $J\ kg^{-1}$) [10]. The $Gd_{20}Ho_{20}Er_{20}Al_{20}Co_{20}$ HE-MG microwire has the lower $|\Delta S_M^{pk}|$ and larger δT_{FWHM} values as compared to its bulk counterparts. Because the microwire has larger cooling speed during the preparation process as compared to the case in the bulk counterpart, the more irregular structure can widen the magnetic-transition temperature range, which is beneficial to its application in the magnetic refrigerators.

The $|\Delta S_M^{pk}|$, δT_{FWHM} and RC_{FWHM} values of the $Gd_{20}Ho_{20}Er_{20}Al_{20}TM_{20}$ HE-MG microwire are shown in Fig. 5. The sample of TM = Co has the largest $|\Delta S_M^{pk}|$ value under the applied field from 1 to 5 T. It is notable that all these alloys have much larger δT_{FWHM} values than the values of other alloys listed in Table 1. The sample of TM = Fe has the largest δT_{FWHM} value of 88 K. The high δT_{FWHM} value is ascribed to the spin glass transition, and the complicated compositions in these HE-MG microwires [10]. The complicated compositions that deviate from the eutectic points, and the high mixing entropy may cause the microstructure heterogeneity, and the fluctuation of the exchange integral of MGs [15], which leads to the magnetic-transition temperature range to be widened. According to the mean-field theory, the $|\Delta S_M^{pk}|$ and RC values can be approximately expressed as power-law relations, i.e., $\Delta S_M^{pk}| \propto H^n$ and $RC \propto H^N$ [35]. The exponents, n and N, dominated by the critical exponents of the alloys, can be extracted from fitting the experimental data in Fig. 5a and c based on the above power-law relations. For the sample of TM = Fe: $n = 0.94$, and $N = 1.02$; the sample of TM = Co: $n = 0.83$, and $N = 1.09$; the sample of TM = Ni: $n = 0.95$, and $N = 1.37$. It is apparent that the $Gd_{20}Ho_{20}Er_{20}Al_{20}Co_{20}$ HE-MG microwire has the largest n and N, which means that the $|\Delta S_M^{pk}|$ and RC_{FWHM} values of this HE-MG microwire can increase most rapidly with increasing the magnetic field in three HE-MG microwires. Therefore, if the high magnetic field was taken into consideration, the $Gd_{20}Ho_{20}Er_{20}Al_{20}Co_{20}$ HE-MG microwire could possess the best magnetocaloric properties, and accordingly is the most suitable for the magnetic refrigerant in the current three HE-MG microwires.

In summary, the $Gd_{20}Ho_{20}Er_{20}Al_{20}TM_{20}$ HE-MG microwires are fabricated successfully. These microwires exhibit the second-order magnetic-phase transition with good magnetocaloric properties. The

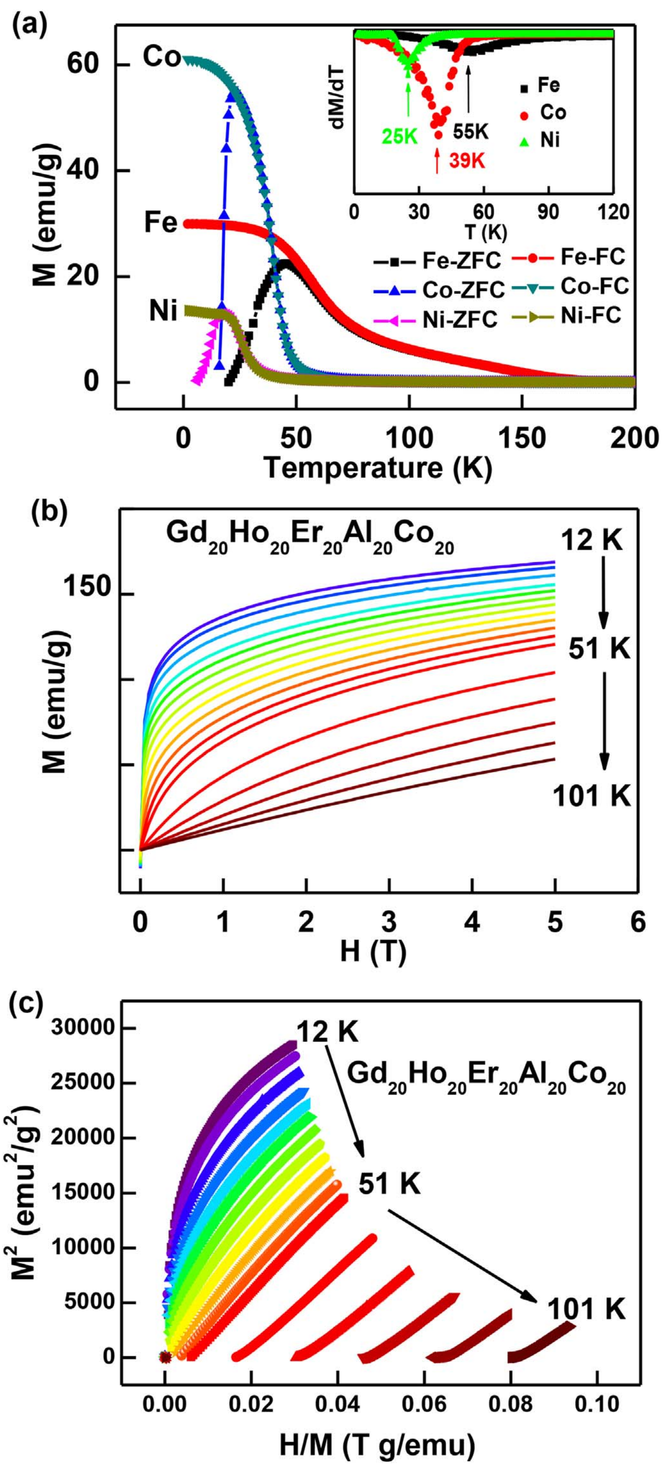

Fig. 3. (a) Temperature dependence of the zero field cooling (ZFC) and field cooling (FC) magnetization under a magnetic field of 200 Oe for $Gd_{20}Ho_{20}Er_{20}Al_{20}TM_{20}$ (TM = Fe, Co and Ni) HE-MG microwires. (b) Isothermal magnetization curves and (c) Arrott plots for $Gd_{20}Ho_{20}Er_{20}Al_{20}Co_{20}$ HE-MG microwires measured at temperatures between 12 and 101 K.

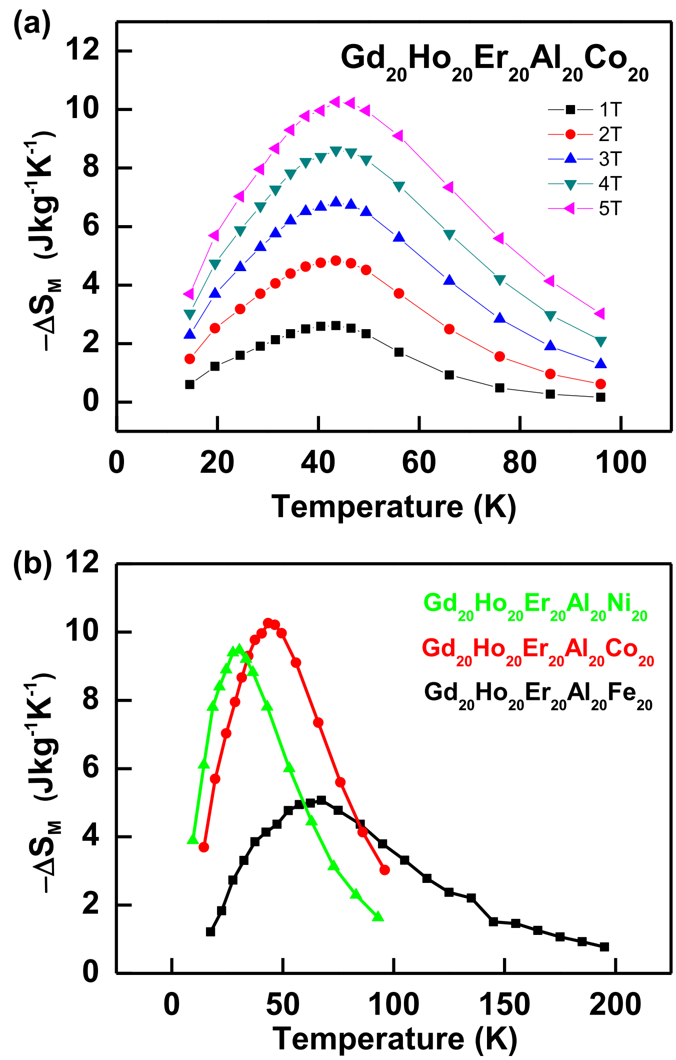

Fig. 4. Magnetic-entropy changes as a function of temperature under the magnetic fields of (b) 1, 2, 3, 4 and 5 T for $Gd_{20}Ho_{20}Er_{20}Al_{20}Co_{20}$ HE-MG microwires, and (c) 5 T for $Gd_{20}Ho_{20}Er_{20}Al_{20}TM_{20}$ (TM = Fe, Co and Ni) HE-MG microwires.

$|\Delta S_M^{pk}|$ and RC_{FWHM} values can reach 10.2 J kg^{-1}K^{-1} and 625 J kg^{-1} under 5 T, respectively, which are significantly larger than those of most rare-earth based MGs. The magnetic-transition temperature can be tuned from 25 to 55 K by alloying different transition elements. Compared with the bulk counterpart, the microwire has a larger δT_{FWHM} value. Therefore, combined with high heat-exchange efficiency of micro-sized wire, the HE-MG microwires are excellent candidates for the magnetic refrigerants.

This work was supported by the National Natural Science Foundation of China (Grant No. 51771217, 51771216) and the Zhejiang Provincial Natural Science Foundation of China (Grant No. LY17E010005, LR18E010002).

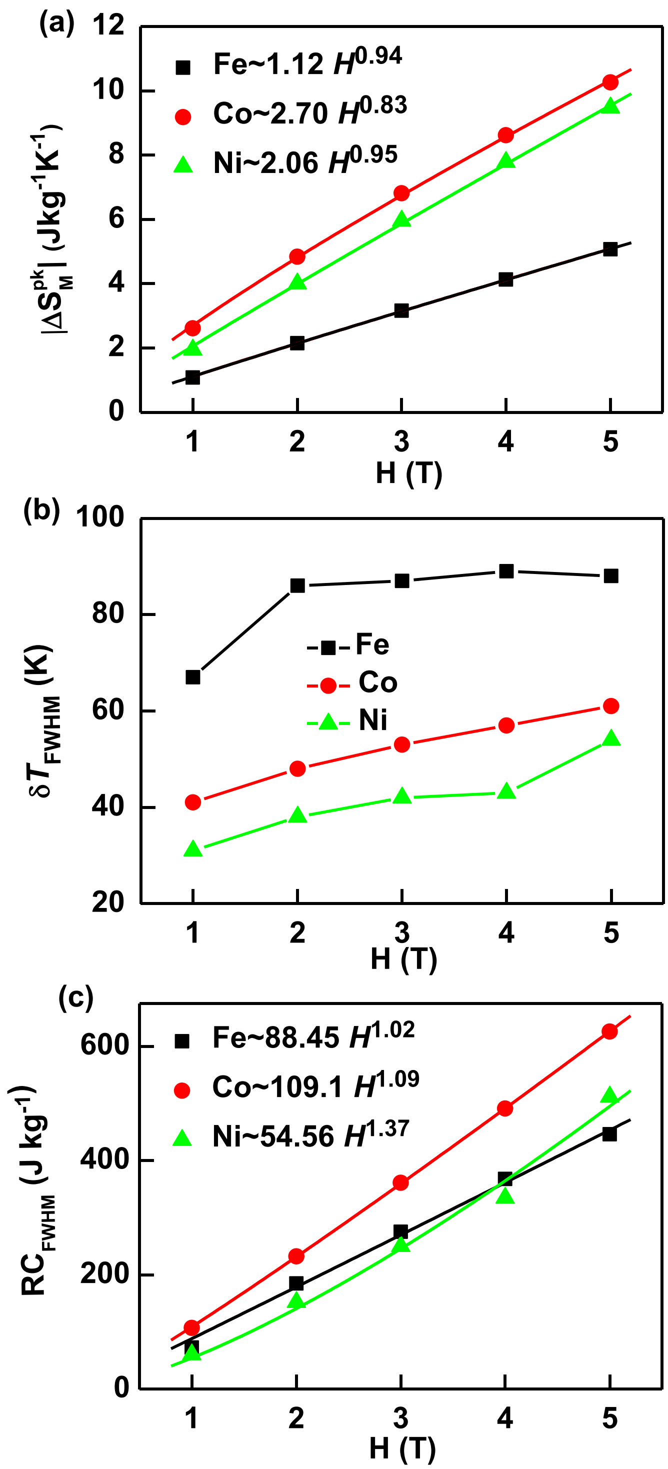

Fig. 5. Magnetic-field dependence of (a) Peak value of the magnetic-entropy. The solid curves are power-law fitting results. (b) Full width at half-maximum of the peak. The solid curves are plotted for guiding eyes. (c) Refrigerant capacity of $Gd_{20}Ho_{20}Er_{20}Al_{20}TM_{20}$ (TM = Fe, Co and Ni) HE-MG microwires. The solid curves are power-law fitting results.

References

[1] S. Gupta, K.G. Suresh, Review on magnetic and related properties of RTX compounds, J. Alloy. Comp. 618 (2015) 562–606.

[2] F.X. Hu, B.G. Shen, J.R. Sun, Z.H. Cheng, G.H. Rao, X.X. Zhang, Influence of negative lattice expansion and metamagnetic transition on magnetic entropy change in the compound $LaFe_{11.4}Si_{1.6}$, Appl. Phys. Lett. 78 (2001) 3675–3677.

[3] X. Moya, L.E. Hueso, F. Maccherozzi, A.I. Tovstolytkin, D.I. Podyalovskii, C. Ducati, L.C. Phillips, M. Ghidini, O. Hovorka, A. Berger, M.E. Vickers, E. Defay, S.S. Dhesi, N.D. Mathur, Giant and reversible extrinsic magnetocaloric effects in $La_{0.7}Ca_{0.3}MnO_3$ films due to strain, Nat. Mater. 12 (2013) 52–58.

[4] K.A. Gschneidner Jr., V.K. Pecharsky, A.O. Tsokol, Recent developments in magnetocaloric materials, Rep. Prog. Phys. 68 (2005) 1479–1539.

[5] K.A. Gschneidner Jr., V.K. Pecharsky, A.O. Pecharsky, C.B. Zimm, Recent developments in magnetic refrigeration, Mater. Sci. Forum 315–317 (1999) 69–76.

[6] H.Y. Ding, Y. Shao, P. Gong, J.F. Li, K.F. Yao, A senary TiZrHfCuNiBe high entropy bulk metallic glass with large glass-forming ability, Mater. Lett. 125 (2014) 151–153.

[7] Y. Zhang, T.T. Zuo, Z. Tang, M.C. Gao, K.A. Dahmen, P.K. Liaw, Z.P. Lu, Microstructures and properties of high-entropy alloys, Prog. Mater. Sci. 61 (2014) 1–93.

[8] M. Yang, X.J. Liu, H.H. Ruan, Y. Wu, H. Wang, Z.P. Lu, High thermal stability and sluggish crystallization kinetics of high-entropy bulk metallic glasses, J. Appl. Phys. 119 (2016) 245112.

[9] Y.F. Ye, Q. Wang, J. Lu, C.T. Liu, Y. Yang, High-entropy alloy: challenges and prospects, Mater. Today 19 (2016) 349–362.

[10] J.T. Huo, L. Huo, J. Li, H. Men, X. Wang, A. Inoue, C. Chang, J.Q. Wang, R.W. Li, High-entropy bulk metallic glasses as promising magnetic refrigerants, J. Appl. Phys. 117 (2015) 073902.

[11] J.T. Huo, L. Huo, H. Men, X. Wang, A. Inoue, J. Wang, C. Chang, R.W. Li, The magnetocaloric effect of Gd-Tb-Dy-Al-M (M = Fe, Co and Ni) high-entropy bulk metallic glasses, Intermetallics 58 (2015) 31–35.

[12] D.D. Belyea, M.S. Lucas, E. Michel, J. Horwath, C.W. Miller, Tunable magnetocaloric effect in transition metal alloys, Sci. Rep. 5 (2015) 15755.

[13] J.D. Dong, A.R. Yan, J. Liu, J. Microstructure and magnetocaloric properties of melt-extracted La–Fe–Si microwires, J. Magn. Magn Mater. 357 (2014) 73–76.

[14] H.Y. Zhang, R. Li, L.L. Zhang, T. Zhang, Tunable magnetic and magnetocaloric properties in heavy rare-earth based metallic glasses through the substitution of similar elements, J. Appl. Phys. 115 (2014) 133903.

[15] Q. Luo, D.Q. Zhao, M.X. Pan, W.H. Wang, Magnetocaloric effect in Gd-based bulk metallic glasses, Appl. Phys. Lett. 89 (2006) 081914.

[16] D. Mishra, M. Gurram, A. Reddy, A. Perumal, P. Saravanan, A. Srinivasan, Enhanced soft magnetic properties and magnetocaloric effect in B substituted amorphous Fe-Zr alloy ribbons, Mater. Sci. Eng. B 175 (2010) 253–260.

[17] F. Wang, T.F. Feng, R.B. Sun, S. Yu, J.Z. Wang, Magnetocaloric effect and critical behavior in amorphous ribbons $Gd_{54}Ho_6Co_{25}Al_{14}Si$, IEEE T. Magn. 51 (2015) 1–4.

[18] Q. Luo, F. Ye, C. Huang, J. Jiao, A. Rahman, P. Yu, J. Li, J. Shen, Size-dependent structure and magnetocaloric properties of Fe-based glass-forming alloy powders, AIP Adv. 6 (2016) 045002.

[19] D.V.M. Repaka, V. Sharma, R.V. Ramanujan, Near room temperature magnetocaloric properties and critical behavior of binary Fe_xCu_{100-x} nanoparticles, J. Alloy. Comp. 690 (2017) 575–582.

[20] F.X. Qin, N.S. Bingham, H. Wang, H.X. Peng, J.F. Sun, V. Franco, S.C. Yu, H. Srikanth, M.H. Phan, Mechanical and magnetocaloric properties of Gd-based amorphous microwires fabricated by melt-extraction, Acta Mater. 61 (2013) 1284–1293.

[21] H. Shen, H. Wang, L. Jingshun, F. Cao, F. Qin, D. Xing, D. Chen, Y. Liu, J. Sun, Enhanced magnetocaloric properties of melt-extracted GdAlCo metallic glass microwires, J. Magn. Magn Mater. 372 (2014) 23–26.

[22] H. Shen, H. Wang, J. Liu, D. Xing, F. Qin, F. Cao, D. Chen, Y. Liu, J. Sun, Enhanced magnetocaloric and mechanical properties of melt-extracted $Gd_{55}Al_{25}Co_{20}$ microfibers, J. Alloy. Comp. 603 (2014) 167–171.

[23] D. Xing, H. Shen, J. Liu, H. Wang, F. Cao, F. Qin, D. Chen, Y. Liu, J. Sun, Magnetocaloric effect in uncoated $Gd_{55}Al_{20}Co_{25}$ amorphous wires, Mater. Res. 18 (2015) 49–54.

[24] Y. Tokal, M. Sahashi, US006022486A, 2000.

[25] J.M. Seuntjens, US005897963A, 1999.

[26] N. Scheerbaum, O. Heczko, J. Liu, D. Hinz, L. Schultz, O. Gutfleisch, N. J. Phys. 10 (2008) 073002.

[27] Z.P. Lu, H. Tan, Y. Li, S.C. Ng, The correlation between reduced glass transition temperature and glass forming ability of bulk metallic glasses, Scripta Mater. 42 (2000) 667–673.

[28] D. Sherrington, S. Kirkpatrick, Solvable model of a spin-glass, Phys. Rev. Lett. 35 (1975) 1792–1796.

[29] Q. Luo, D.Q. Zhao, M.X. Pan, W.H. Wang, Magnetocaloric effect of Ho-, Dy-, and Er-based bulk metallic glasses in helium and hydrogen liquefaction temperature range, Appl. Phys. Lett. 90 (2007) 211903.

[30] C. Mayer, S. Gorsse, G. Ballon, R. Caballero-Flores, V. Franco, B. Chevalier, Tunable magnetocaloric effect in Gd-based glassy ribbons, J. Appl. Phys. 110 (2011) 053920.

[31] J. Fan, L. Ling, B. Hong, L. Zhang, L. Pi, Y. Zhang, Critical properties of the perovskite manganite $La_{0.1}Nd_{0.6}Sr_{0.3}MnO_3$, Phys. Rev. B 81 (2010) 144426.

[32] V. Franco, J.S. Blázquez, A. Conde, Field dependence of the magnetocaloric effect in materials with a second order phase transition: a master curve for the magnetic entropy change, Appl. Phys. Lett. 89 (2006) 222512.

[33] N.S. Bingham, A.K. Suszka, C.A.F. Vaz, H. Kim, L.J. Heyderman, Interfacial room temperature magnetism and enhanced magnetocaloric effect in strained $La_{0.66}Ca_{0.34}MnO_3/BaTiO_3$ heterostructures, Phys. Rev. B 96 (2017) 024419.

[34] C.M. Bonilla, F. Bartolomé, L.M. García, M. Parra-Borderías, J. Herrero-Albillos, V. Franco, A new criterion to distinguish the order of magnetic transitions by means of magnetic measurements, J. Appl. Phys. 107 (2010) 09E131.

[35] J.Y. Law, V. Franco, R.V. Ramanujan, Influence of La and Ce additions on the magnetocaloric effect of Fe-B-Cr-based amorphous alloys, Appl. Phys. Lett. 98 (2011) 192503.